Electronic Supplementary Material (ESI) for Physical Chemistry Chemical Physics.

Excimers from Stable and Persistent Supramolecular Radical-Pairs in Red/NIR-Emitting Organic Nanoparticles and Polymeric Films

Davide Blasi,[a] Domna Maria Nikolaidou,[b] Francesca Terenziani,[b]* Imma Ratera,[a]* Jaume Veciana[a]

Supplementary Information

Synthesis of Molecules and Preparation of Organic Nanoparticles (ONPs)

TTM-αH and TTM radical were synthesized following a procedure reported in literature.[1,2]

Pure TTM radical nanoparticles were prepared following the reprecipitation method. A 2 mM solution of the radical compound in THF was prepared; 100 µL of this stock solution were injected into 9.9 mL of MilliQ water under vigorous stirring (1000 rpm) at room temperature for 30 minutes (the final nominal concentration of radical is 10^{-5} M; the water/THF ratio is 99/1 V/V).

Radical-doped ONPs were prepared in a similar way. 2 mM solutions of TTM-αH containing different amounts of TTM radical (0.5%, 3%, 6.5%, 13%, 26%, 50 % in mol.) in THF were prepared and filtered over 220 nm Teflon filters. 100 µL of each solution were slowly dropped in 9.9 mL of MilliQ water at room temperature under vigorous stirring (1000 rpm) for 30 minutes.

Preparation of PMMA films

Different stock solutions were prepared with various ratio of PMMA and TTM radical. PMMA (Sigma-Aldrich m.w.= 960000 g mol^{-1}) was dissolved in Chloroform (Tecknokroma, HPLC grade) 10% w/w, then the radical was added in specific ratio: 1%, 5%, 10%, 15% & 20% (w/w). For the deposition, 80 µL of solution were drop-casted on a quartz substrate. When the solution was dry, films were stabilized under vacuum at room temperature for 4h.

[a] Mr. D. Blasi, Dr. I. Ratera, Prof. J. Veciana
Institut de Ciència de Materials de Barcelona (CSIC)/CIBER-BBN
Campus de la UAB, E-08193 Bellaterra, Barcelona, Spain
E-mail: iratera@icmab.es
[b] Mr. D. M. Nikolaidou, Dr. F. Terenziani
Chemistry Department, University of Parma & INSTM-UdR Parma,
I-43124, Parma, Italy
E-mail: francesca.terenziani@unipr.it

Spectroscopic Characterization

Absorption spectra were measured with an Agilent UV-Cary 5000 Spectrometer and with a Perkin Elmer Lambda 650 spectrophotometer.

Luminescence spectra were measured with a Horiba Jobin-Yvon Spectrofluorometer Fluoromax-3. Luminescence quantum yields of solutions and of nanoparticles suspensions were evaluated using Cresyl Violet perchlorate in MeOH (LQY=0.54)[3] as the reference. Luminescence quantum yields of the films were evaluated with a Horiba Quanta-φ integrating sphere coupled with the Fluoromax-3 Fluorometer, using a film of pure PMMA as the reference scatterer.

For luminescence lifetimes, the Horiba Jobin-Yvon Fluoromax-3 Spectrofluorometer was used in TCSPC (time-correlated single photon counting) mode, with a pulsed NanoLED @ 370 nm as the excitation source. The decays were fitted either with multi-exponential functions or stretched-exponential functions. The fitting results were judged by the reduced χ^2 value (χ^2 < 1.2).

Photodegradation of the solutions and of ONPs suspensions was evaluated by monitoring the luminescence over time under continuous irradiation of the stirred samples at 375 nm (instrument: Cary Eclipse Fluorescence Spectrophotometer). Emission wavelength was set to 570 nm (monomer-like emission band) or 660 nm (excimer emission band). Luminescence was measured at 5-second time intervals. The THF solution of TTM was prepared as to have the same optical density as the 13% TTMd-ONPs. Both the organic solution and the ONPs suspension were degassed for 15 min bubbling Ar inside the screw-cup quartz cuvettes, under stirring.

Absorption and Emission of TTM radical in THF

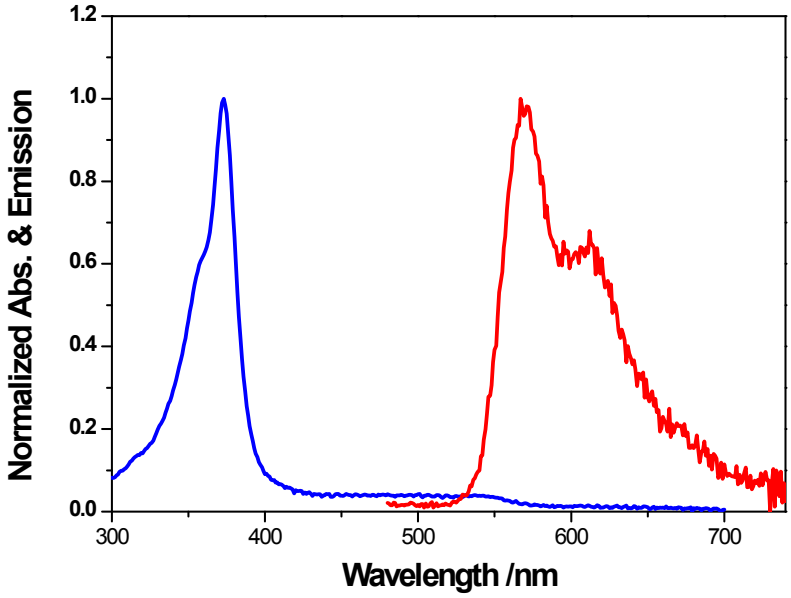

Figure S1. Normalized absorption (blue line) and emission (red line) spectra for TTM radical in THF.

Absorption and Emission of TTM radical in glassy solvent at low temperature

2-Methyl THF was used after drying overnight with molecular sieves type A3 and after filtration with 0.45 µm PTFE filters. All solutions were prepared, sonicated for 1 minute and stocked in the dark. To obtain transparent glassy matrixes, 2-MeTHF solutions were rapidly cooled (about 20 K per minute) to 77 K with an Oxford Instruments OptistatDN cryostat providing a controlled low-temperature exchange gas environment for the sample contained in quartz cuvettes specially designed for cryogenics.

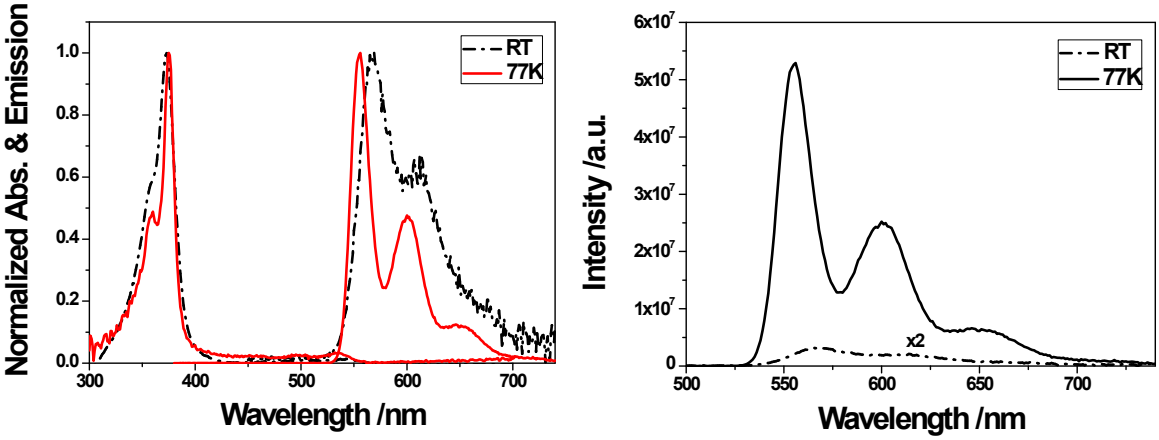

Figure S2. Left panel: Normalized absorption and emission spectrum of TTM in 2-MeTHF at room temperature (dotted lines) and at 77 K (red lines). Right panel: Comparison of the intensity of fluorescence of TTM at room temperature (dotted line) vs 77 K (full line).

DLS and TEM Characterization

Dynamic Light Scattering (DLS) and Z-potential measurements were performed at room temperature with a Malvern Nano ZS using equipped with a laser at 633 nm. Each measurement consists in 13 scans and the reported values are the average values of three measurements.

Samples were observed using transmission electron microscopy (TEM) with the aid of negative staining. One drop of the sample was applied to glow-discharged carbon-coated copper grids (SPI) for 3 minutes. Subsequently, one drop of 2% uranyl acetate was placed on the grid for 1-2 min before being drained off. The grid was then placed in a transmission electron microscope (Jeol JEM 1400) operating at an accelerating voltage of 120 kV. Images were acquired using an Orius SC200 (Gatan).

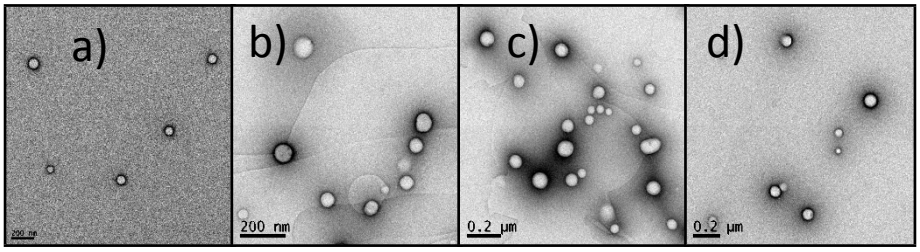

Figure S3. TEM images of a) TTMd-ONPs 3%, b) TTMd-ONPs 6.5%, c) TTMd-ONPs 13%, d) TTMd-ONPs 26% (scale 200 nm).

Correction of scattering in UV-vis spectra of ONPs

The nanoparticle suspension of pure TTM-αH (used as pure scatterer) was prepared with the standard precipitation procedure: a 2 mM THF solution of TTM-αH was prepared and filtered using a 220 nm Teflon filter. 100 µL of this solution were slowly dropped in 9.9 mL of MilliQ water at room temperature under vigorous stirring (1000 rpm). The absorption spectrum of this suspension dominated by scattering in the 280-900 nm range (TTM-αH does not absorb in this region). The scattering signal has been fitted, modified in order to match with the scattering of each sample and then subtracted to each of the TTMd-ONPs suspensions.

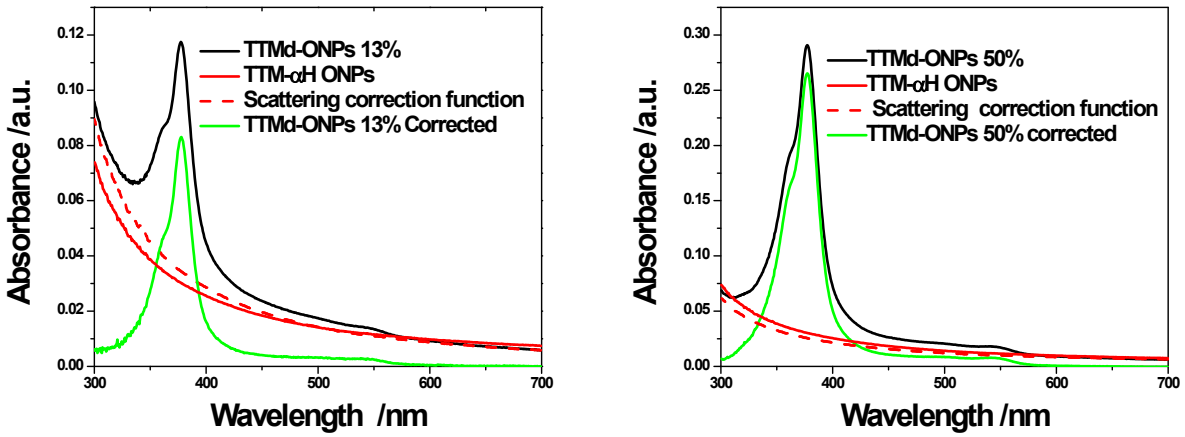

Figure S4. Absorbance correction of the 13% and 50% TTMd-ONPs samples. Recorded spectrum of TTMd-ONPs (black); recorded spectrum of TTM-αH ONPs (red); scattering-correction fitting curve (dashed-red); absorption spectrum of TTMd-ONPs after correction (green).

Steady-state Fluorescence of TTMd-ONPs

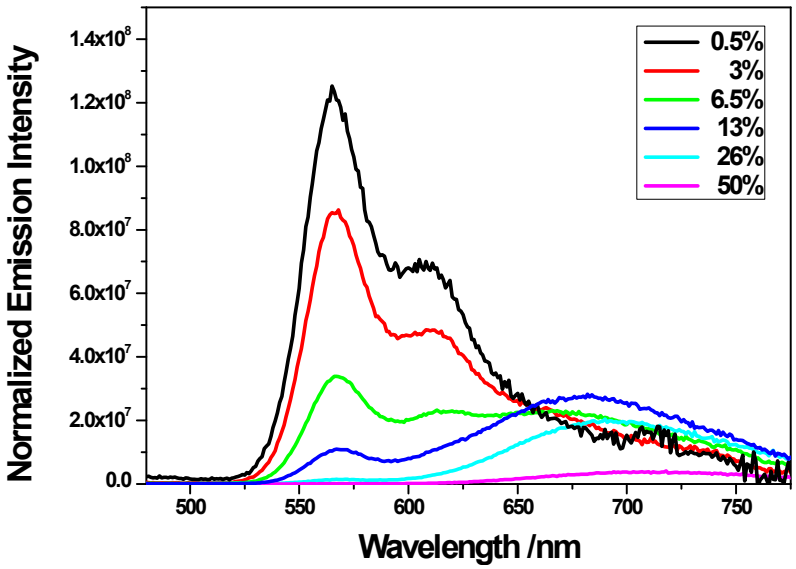

Figure S5. Emission spectra of TTMd-ONPs normalized with respect to the absorbance of each sample (so that the area of each spectrum is proportional to the LQY).

The monomer's and excimer's emission intensities (I_M and I_E, respectively) are given by:[4,5]

$$I_M \propto n_{abs} k_r \tau_M \qquad \text{(eq. S1)}$$

$$I_E \propto n_{abs} f k_r^{'} \tau_E \propto n_{abs} k_E \tau_M k_r^{'} \tau_E \qquad \text{(eq. S2)}$$

where n_{abs} is the number of absorbed photons (typically proportional to the fluorophore concentration); k_r and $k_r^{'}$ are the radiative emission rates of the monomer and of the excimer, respectively; τ_M and τ_E are the emission lifetimes associated to the monomer and to the excimer, respectively; f is the fraction of excited monomers converted into excimers. This last factor is given by the ratio between the formation rate of the excimer (k_E) and the sum of the rates depopulating the monomer excited state (τ_M^{-1}). In the case of diffusion-driven excimer formation, k_E is usually proportional to the fluorophore concentration, while a very different dependence on concentration can be expected in other cases: for example, in the case of intramolecular excimers (where no translation is needed) k_E can be assumed as independent of the concentration.[5]

Expressions (1) and (2) lead to estimate the excimer/monomer (E/M) emission ratio as:

$$\frac{I_E}{I_M} = \frac{k_r^{'}}{k_r} k_E \tau_E \qquad \text{(eq. S3)}$$

In the case of our TTMd-ONPs, the observed E/M emission ratio increases roughly quadratically with respect to the concentration (at least up to the 26%-doped sample): since a slightly more than linear dependence is accounted for by the excimer lifetime (Table 2), we expect k_E to increase less than linearly with the fluorophore concentration.

It is interesting to discuss these results in relation to the specific observed intensities of monomer and excimer emission. In Figure S5 the emission intensity is reported as normalized with respect to n_{abs} (i.e. to the absorbance of each sample), as to better discuss the non-trivial dependence of the intensities on the fluorophore concentration. I_M/n_{abs} decreases with increasing concentration, suggesting an almost linear decrease of $k_r\tau_M$, in agreement with the measured decrease of τ_M. At the same time, I_E/n_{abs} increases (less than linearly) with the concentration up to the 13%-doping: since the decrease in τ_M roughly compensate the increase of τ_E, the dependence of I_E/n_{abs} on the concentration is mostly governed by k_E. The estimated less-than-linear increase of k_E with concentration thus explains the dependence of I_E/n_{abs} on the fluorophore concentration. For higher TTM radical concentration (already starting from the 26% TTMd-ONPs) the excimer emission is affected by ACQ, leading to a complete loss of luminescence in the pure TTM samples (either powders or ONPs).

Table S1. Results of the three-exponential fitting (corresponding lifetimes τ_1, τ_2, τ_3 and relative amplitudes) and of the stretched-exponential fitting (lifetime τ_0 and stretch factor β) of the luminescence decays of the TTMd-ONPs at the emission wavelength of the monomer (M) and/or of the excimer (E).

		λ_{em} [nm]	3-exp fit			stretched-exp fit	
			τ_1 [s]	τ_2 [s]	τ_3 [s]	τ_0 [s]	β
TTMd-ONPs	0.5%	570 (M)	1.5×10^{-7} (28.67)	5.6×10^{-7} (69.63)	2.2×10^{-8} (1.7)	1.5×10^{-7}	0.60
	3%	570 (M)	1.1×10^{-7} (42.80)	5.0×10^{-7} (52.91)	2.2×10^{-8} (4.29)	5.7×10^{-8}	0.56
	6.5%	570 (M)	4.7×10^{-8} (33.03)	4.0×10^{-7} (63.24)	1.8×10^{-9} (3.74)	1.1×10^{-8}	0.35
		670 (E)	8.7×10^{-8} (18.51)	6.6×10^{-7} (76.61)	1.6×10^{-8} (4.88)	4.9×10^{-9}	0.25
	13%	570 (M)	2.8×10^{-8} (15.46)	4.3×10^{-7} (78.16)	2.2×10^{-9} (6.38)	2.1×10^{-9}	0.38
		680 (E)	3.9×10^{-8} (3.17)	8.1×10^{-7} (95.84)	6.8×10^{-9} (1.00)	1.3×10^{-8}	0.23
	26%	570 (M)	6.0×10^{-8} (10.85)	5.1×10^{-7} (82.94)	1.0×10^{-9} (6.21)	1.6×10^{-9}	0.26
		700 (E)	1.0×10^{-7} (4.41)	8.7×10^{-7} (95.29)	3.5×10^{-9} (0.3)	5.4×10^{-7}	0.64
	50%	720 (E)	6.0×10^{-8} (6.43)	9.2×10^{-7} (91.81)	4.6×10^{-9} (1.76)	1.5×10^{-9}	0.24

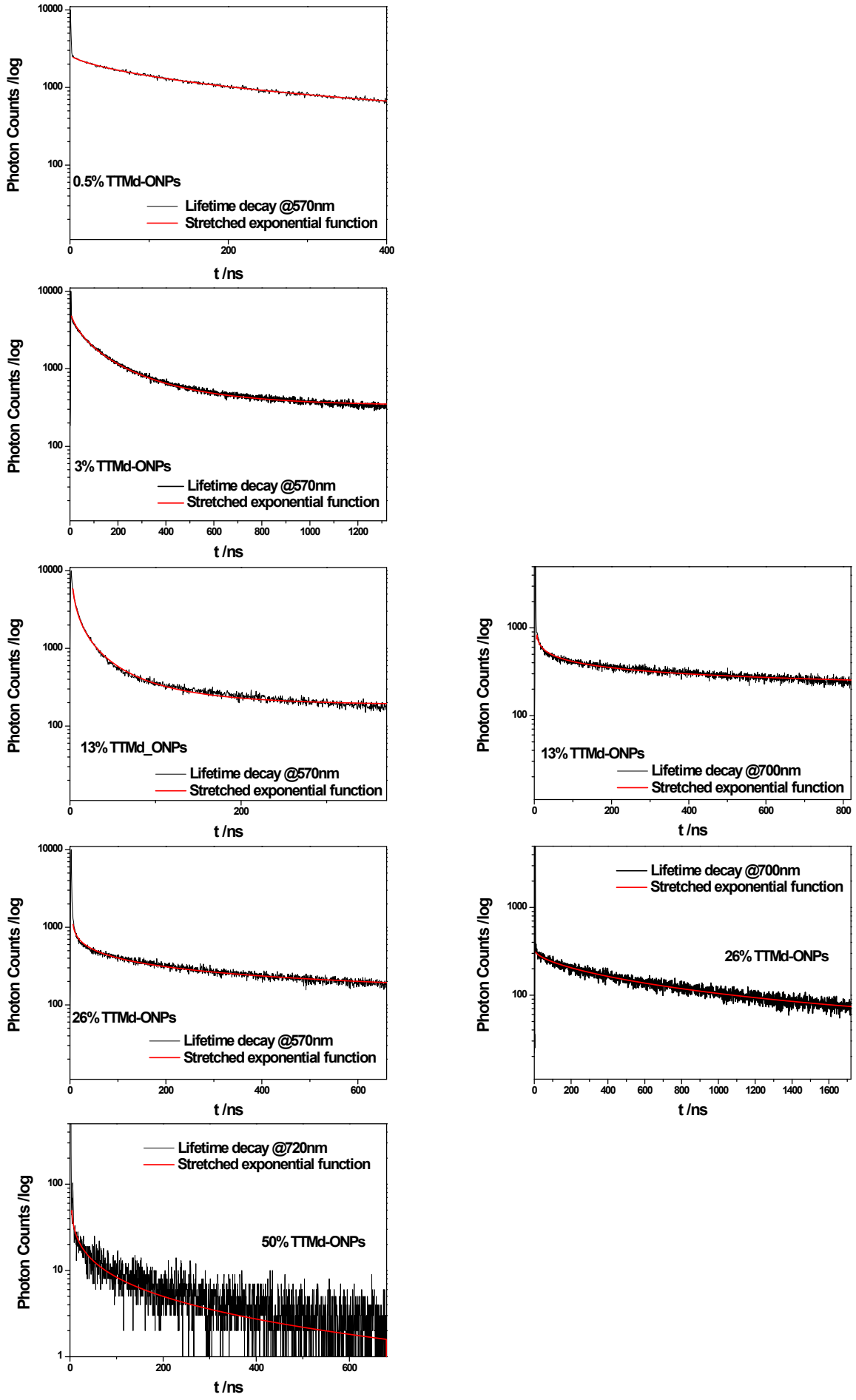

Figure S6. Luminescence decays and corresponding stretched-exponential fits, for TTMd-ONPs.

Luminescence spectra of TTMd-PPMA films

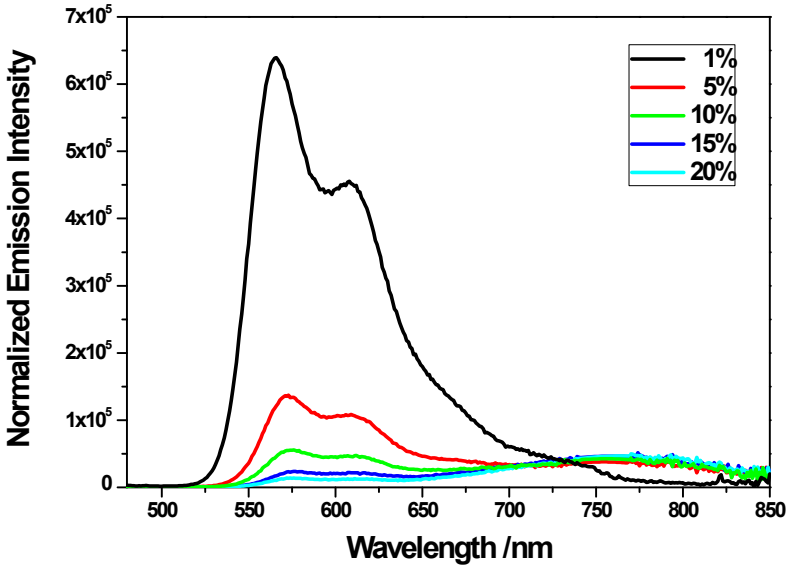

Figure S7. Raw luminescence spectra of TTMd-PMMA, each divided by the corresponding absorbance as evaluated via the integrating sphere (area is proportional to the LQY).

Table S2. Results of the three-exponential fitting (corresponding lifetimes τ_1, τ_2, τ_3 and relative amplitudes) and of the stretched-exponential fitting (lifetime τ_0 and stretch factor β) of the luminescence decays of the TTMd-PMMA films at the emission wavelength of the monomer (M) and/or of the excimer (E).

TTMd-film	λ_{em} [nm]	3-exp fit			stretched-exp fit	
		τ_1 [s]	τ_2 [s]	τ_3 [s]	τ_0 [s]	β
1%	570 (M)	1.5×10^{-8} (5.91)	9.1×10^{-8} (50.73)	3.7×10^{-7} (6.86)	4.52×10^{-8}	0.56
5%	570 (M)	5.7×10^{-8} (26.05)	4.8×10^{-7} (66.78)	8.1×10^{-9} (7.17)	1.9×10^{-8}	0.52
10%	570 (M)	2.3×10^{-8} (52.60)	8.5×10^{-8} (30.50)	4.0×10^{-9} (16.9)	3.5×10^{-9}	0.43
	750 (E)	7.9×10^{-8} (17.12)	5.8×10^{-7} (76.45)	1.1×10^{-8} (6.43)	3.3×10^{-11}	0.15
15%	570 (M)	1.9×10^{-8} (36.91)	2.1×10^{-7} (48.86)	3.4×10^{-9} (14.24)	2.2×10^{-11}	0.16
	750 (E)	1.8×10^{-7} (8.92)	8.2×10^{-7} (90.76)	1.1×10^{-8} (0.32)	5.0×10^{-7}	0.76
20%	570 (M)	6.0×10^{-8} (10.85)	5.1×10^{-7} (82.94)	1.0×10^{-9} (6.21)	7.2×10^{-9}	0.24
	750 (E)	5.3×10^{-9} (1.22)	6.2×10^{-7} (87.38)	2.0×10^{-7} (11.40)	6.3×10^{-8}	0.32

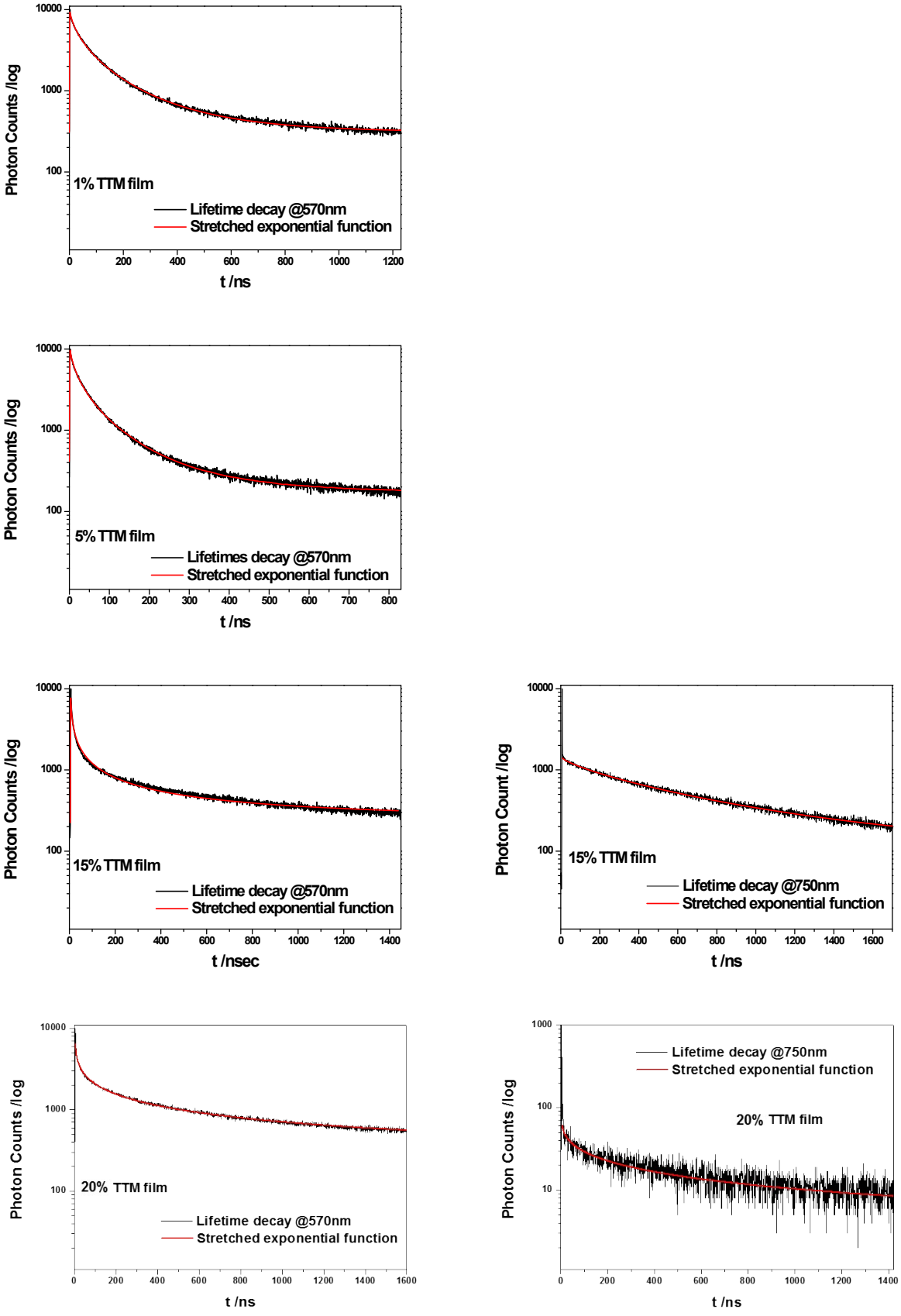

Figure S8. Luminescence decays and corresponding stretched-exponential fits, for TTMd-PMMA films.

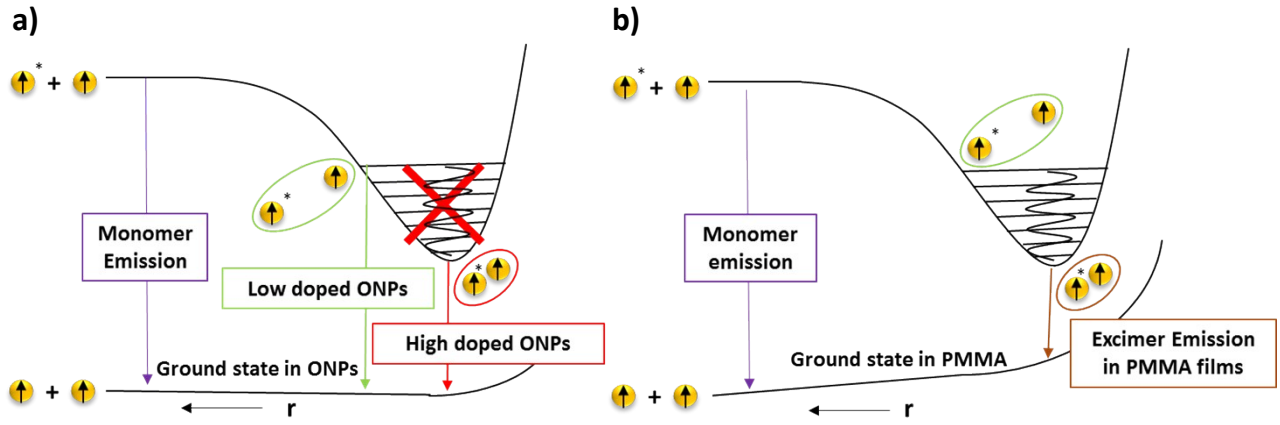

Figure S9. Representation of the excimer formation in ONPs (a) and PMMA films (b). The lower monotonous curve represents the repulsive energy between the two molecules in the ground state. The upper curve, which is relative to two molecules, one being in the ground state and the other in the excited state, exhibits a minimum corresponding to the optimum formation of the excimer. For a rigid matrix (ONPs), the exciton is trapped in more and more stabilized excimer configurations as the fluorophore concentration increases, with a consequent progressive red-shift of the excimer emission (panel a). In less rigid environments (films), relaxation allows the excimer to achieve the most stable configuration, quite independently of the concentration (panel b).

References

(1) Ballester, M.; Riera, J.; Castaner, J.; Rovira, C.; Armet, O. *Synthesis (Stuttg).* **1986**, *1*, 64–66.

(2) O. Armet, J. Veciana, C. Rovira, J. Riera, J. Castañer, E. Molins, J. Rius, C. Miravitlles, S. Olivella, J. B. *J. Phys. Chem.* **1987**, *91*, 5608–5616.

(3) Magde, D.; Brannon, J. H.; Cremers, T. L.; Olmsted, J. *J. Phys. Chem.* **1979**, *83* (6), 696–699.

(4) J. R. Lakowicz, *Principles of fluorescence spectroscopy*, 2006. Springer Science+Buisness Media, LLC.

(5) B. Valeur, *Molecular Fluorescence Principles and Applications*, 2001, vol. Wiley-VCH.